Multi-Drug Resistance Transporter 2 Regulates Mucosal Inflammation by Facilitating the Synthesis of Hepoxilin A₃

Michael Pazos[†], **Dario Siccardi**[†,¥], **Karen L. Mumy**[†,¥], **Jeffrey D. Bien**[†], **Steve Louie**[†], **Hai Ning Shi**[†], **Karsten Gronert**[#], **Randall J. Mrsny**[‡,¢], and **Beth A. McCormick**[†,¥,*]

[†]*Department of Pediatric Gastroenterology and Nutrition, Massachusetts General Hospital, Boston, MA 02129* [¥]*Department of Microbiology & Molecular Genetics, Harvard Medical School, 200 Longwood Ave., Boston, MA 02115* [#]*University of California, Berkeley, Center for Eye Disease and Development, School of Optometry, Berkeley, CA.94720* [‡]*Department of Pharmacy & Pharmacology, University of Bath, Claverton Down, Bath, BA2 7AY, England* [¢]*Unity Pharmaceuticals, 1455 Adams Drive, Suite 1150, Menlo Park, CA 94025*

Abstract

Neutrophil transmigration across mucosal surfaces contributes to dysfunction of epithelial barrier properties, a characteristic underlying many mucosal inflammatory diseases. Thus, insight into the directional movement of neutrophils across epithelial barriers will provide important information relating to the mechanisms of such inflammatory disorders. The eicosanoid hepoxilin A₃, an endogenous product of 12-lipoxygenase activity, is secreted from the apical surface of the epithelial barrier and establishes a chemotatic gradient to guide neutrophils from the submucosa, across epithelia to the luminal site of an inflammatory stimulus - the final step in neutrophil recruitment. Currently, little is known regarding how hepoxilin A₃ is secreted from the intestinal epithelium during an inflammatory insult. In this study we reveal that hepoxilin A₃ is a substrate for the apical efflux ABC transporter, multi-drug resistance protein 2 (MRP2). Moreover, using multiple *in vitro* and *in vivo* models we show that induction of intestinal inflammation profoundly up-regulates apical expression of MRP2, and that interfering with hepoxilin A₃ synthesis and/or inhibition of MRP2 function results in a marked reduction in inflammation and severity of disease. Lastly, examination of inflamed intestinal epithelia in human biopsies revealed up-regulation of MRP2. Thus, blocking hepoxilin A₃ synthesis and/or inhibiting MRP2 may lead to the development of new therapeutic strategies for the treatment of epithelial-associated inflammatory conditions.

Introduction

Transmigration of neutrophils (PMNs) across epithelial surfaces represents a shared phenomenon among a diverse array of inflammatory mucosal conditions. For example, salmonellosis, shigellosis, and pneumonia, as well as autoimmune/idiopathic states such as Crohn's disease, ulcerative colitis, bronchitis, chronic obstructive pulmonary disease, and oral diseases such as periodontitis all culminate in the destructive breach of the protective outer epithelium by activated PMNs. Furthermore, the severity and clinical outcome of these inflammatory diseases correlate with the extent of PMN infiltration (8,12). An emerging

[*]**Corresponding Author:** Beth A. McCormick, Ph.D. Massachusetts General Hospital CNY 114 16th Street (3503) Charlestown, MA 02129 U.S.A. TEL: 617-726-4168 FAX: 617-726-4172 e-mail: mccormic@helix.mgh.harvard.edu

concept over the past decade suggests an orchestrated movement of PMNs from the bloodstream to luminal sites of inflammatory stimuli. For example, in response to inflammatory stimuli within the intestinal lumen, IL-8, as well as other CXC chemokines, are secreted from the basolateral surface of enterocytes prompting PMN escape from the bloodstream and eventual accumulation within the submucosal space (1). In concert, the potent PMN chemoattractant, hepoxilin A$_3$ (HXA$_3$), is secreted from the apical surface of the epithelial barrier where it establishes a chemotactic gradient to guide PMNs from the submucosa across the epithelium, a process constituting the final step in PMN recruitment to the mucosal lumen (2). HXA$_3$ is a hydroxy epoxide metabolite formed from the intermediate 12S-hydroperoxyeicosa-5Z,8Z,10*E*,14*Z*-tetraenoic acid (12*S*-HpETE), the main product of 12S-lipoxygenase activity (3,4) (5). Hepoxilin synthase activity, responsible for the conversion of 12-S-HETE to HXA$_3$, has been confirmed for human platelet 12-LOX, human epidermal LOX type 3 and murine and porcine 12/15-LOX (5,6). Recently, a critical role for HXA$_3$ in PMN-mediated events in both intestinal and pulmonary inflammation has been demonstrated (2, 7-9).

To perform its specific function of drawing PMNs into a mucosal lumen, HXA$_3$ must be secreted from the apical surface of epithelial cells thereby establishing a concentration gradient across epithelial tight junctions to incite paracellular PMN movement. HXA$_3$ performs this function as a pure chemoattractant that does not induce neutrophil activation (10), leaving that event to occur in the presence of pathogens and other stimuli following arrival at the epithelial luminal surface (2). Despite the critical nature of PMN transmigration in pathogen elimination and disease pathophysiology, many of the details regarding the regulation of PMN migration across mucosal surfaces remain undefined. Herein, we describe a mechanism for the vectored secretion of HXA$_3$ from the apical surface of epithelial cells involving the ATP binding cassette (ABC) transporter multi-drug resistance associated protein 2 (MRP2). In general, the physiological role of ABC transporters covers a wide spectrum of functions varying from the transport of excretory compounds and toxins, to the elimination of xenobiotics (11). Our findings reveal a previously unappreciated role of MRP2 in mediating the inflammatory response as we demonstrate that inflammatory signals up-regulated MRP2 expression in association with 12-LOX activity, a critical element in the synthesis of HXA$_3$. Furthermore, our studies not only provide vital insight into the contribution of ABC transporters in the pathogenesis of inflammatory disorders of the gastrointestinal tract with respect to mechanisms underlying PMN recruitment but also identify novel targets for the treatment of epithelial-associated inflammatory conditions, such as inflammatory bowel disease (IBD).

Materials and Methods

Cell culture

T84 intestinal epithelial cells (passages 40-58) were grown as previously described (12). For transport experiments T84 cells were seeded at 250,000/cm^2 on inverted polycarbonate membrane Transwell™ inserts (4.5 mm diameter) and cultured at 37°C, 90% relative humidity, and 5% CO$_2$. HCT-8 (at passage 30-40) were seeded on inverted Transwell inserts at a density of 40,000/cm^2 and cultured to day 7-10 post-seeding for efflux experiments. The formation of restrictive monolayers (at least 800 ohm.cm^2) was monitored for all cell types by measurement of transepithelial electrical resistance using an EVOM Voltometer (World Precision Instruments, Sarasota, FL, USA).

Growth of bacteria for assays using cell culture inserts

Nonagitated microaerophilic bacterial cultures were prepared as previously described (12). *Salmonella enterica* serotype Typhimurium (*S. typhimurium*) SL1344 (wild-type), EE633

(*sipA*-), AvrA-, VV341 (*hil*A-) as well as *E. coli* F-18 were used in this study and have previously been described (12,13).

PMN transepithelial migration

The PMN transmigration assay using inverted cell culture monolayers of polarized cells has been described previously (12).

ABC transport inhibitors

For experiments involving ABC transport inhibitors, epithelial cells were pre-treated for 1 hr with either cyclosporine A (10-1000 nM), verapamil (0.1-10000 nM), probenecid (10-100 μM) or MK571 (50-100 μM). Following pre-treatment, the drug was removed by washing with Hanks Balanced Salt Solution (HBSS$^+$) containing Mg^{2+}, Ca^{2+}, and 10 mM Hepes (HBSS; pH 7.4) prior to infecting polarized T84 monolayers at the apical surface with wild-type *S. typhimurium* SL1344.

Collection and identification of HXA$_3$ and 12-HETE

Method 1: The apical surface of polarized T84 cell monolayers were infected with *S. typhimurium* SL1344 or EE633 as previously described (2,10). Subsequent HXA3 identification was carried out according to the protocol described by Mrsny et al (2). This method was used to obtain the data shown in Figure 3C.

Method 2: T84 or HCT-8 monolayers grown on 4.5 cm^2 Transwells were drained of media and washed with warm HBSS+ prior to infection with *S. typhimurium* (multiplicity of infection 100:1) for 1 h at 37°C. The bacteria were washed away with warm HBSS+ and 750 μl HBSS + was added to the apical surface, with 2 ml HBSS+ in the basolateral chamber. The Transwells were incubated at 37°C and the buffer in the apical compartment was collected every 2 h and replenished with the same volume of fresh HBSS+. Collected buffer was pooled and stored on ice in the dark. After 6 h (3 collections), all pooled samples received 0.5 ng of prostaglandin B$_2$ (PGB$_2$; Cayman Chemical, Ann Arbor, MI) as an internal standard and was brought to a pH of 3-4 with HCl prior to extraction. Samples were extracted by solid phase as previously described (14). Samples were eluted in 5 ml methanol, concentrated under nitrogen, and resuspended in 100 μl methanol. Samples were stored at −80°C until analyzed.

HXA$_3$ (8-hydroxy-11,12-epoxy-eicosatetraenoic acid) was identified by LC/MS/MS based lipidomic analyses (9,15). Extracted samples suspended in methanol were analyzed by a triple quadruple linear ion trap LC/MS/MS system (MDS SCIEX 3200 QTRAP; Applied Biosystems, Foster City, CA) equipped with a LUNA C18-2 mini-bore column (Phenomenex, Torrance, CA) using a mobile phase (methanol:water:acetate, 65:35:0.03, v:v:v) with a 0.35 ml/flow rate. MS/MS analyses were carried out in negative ion mode and fatty acids were identified and quantified by multiple reaction monitoring (MRM mode) using specific transitions for hepoxilin A$_3$ (335 →127 *m/z*), and 12-HETE (319→179 *m/z*). Specific retention time for HXA$_3$ and 12-HETE was established with a synthetic standard (Biomol, Plymouth Meeting, PA) and transition ions established by MS/MS analyses using enhanced product ion mode with appropriate selection of the parent ion in quadrupole 1 (Q1). Calibration curves (1-1000 pg) for HXA$_3$, 12-HETE, and PGB$_2$ were established with synthetic standards.

Immunoprecipitation studies

T84 or HCT-8 polarized monolayers were apically infected with either wild-type *S. typhimurium* (SL1344), EE633, or the bacterial negative control commensal isolate *E. coli* F-18 (12). Immunoprecipitation was performed using the Seize X Mammalian Immunoprecipitation Kit (Pierce, Rockford, IL) according to manufacturer's instructions. The

bead column was cross-linked with 70 μg of goat anti-MRP2 polyclonal or goat anti-MDR polyclonal antibodies (Santa Cruz Biotechnology, Santa Cruz, CA). Whole cell lysates added to each column were normalized to 0.5 mg per column. Eluted protein was electrophoresed on a non-denaturing gradient SDS-PAGE gel (8-16% Tris-glycine; Cambrex Biosciences, Rockford, ME). Proteins were transferred using a standard semi-dry transfer method onto nitrocellulose and probed with MRP2 or MDR polyclonal antibodies (1:500) overnight at 4° C followed by washes and incubation with horseradish peroxidase-labeled donkey anti-goat antibodies (1:1000; Santa Cruz Biotechnology, Santa Cruz, CA) for 1 h. Bands were detected using SuperSignal West Pico Chemiluminescent Substrate (Pierce, Rockford, IL).

Streptomycin model of acute inflammation

Based on a modification of Barthel et al. (16), female C57 Bl/6 mice, 6-8 weeks old (Jackson Labs, Bar Harbor, ME) were orally treated with 75 μl of streptomycin sulfate (stock 50 mg/ml; Sigma, St. Louis, MO) in sterile distilled water following a 4 h starvation period of both food and water. After 24 h, the mice were starved for 4 h and orally gavaged with 5×10^8 colony-forming units (CFU) of the appropriate bacterial strain in 500 μl of sterile HBSS, monitored for 48 h and sacrificed.

Human intestinal biopsy material

The diagnosis of IBD was based on clinical, endoscopic, and histological criteria, and infectious colitis was ruled out by stool cultures. The collection of samples was approved by the Institutional Review Board at the University of Chicago. Intestinal biopsy specimens were obtained from four ulcerative coltiis and four Crohn's disease patients during routine endoscopy upon informed consent. Control colonic biopsy specimens were obtained from aged and sex matched individuals undergoing surgery for cancer resection.

Slide preparation and hemotoxylin staining

Murine intestinal sections were harvested from the proximal colon of mice at necropsy. Human tissue was obtained from inflamed or non-inflamed biopsy samples of matched patient samples acquired through the Department of Pathology at University of Chicago as a generous gift of Dr. Jerrold R. Turner. All tissues were imbedded in Tissue-Tek OCT compound (Sakura Finetek U.S.A, Torrance, CA), flash-frozen in liquid nitrogen, and sectioned (5 μm thickness) on a 2800 Frigocut cryostate (Reichert-Jung, Germany). Hemotoxylin and Eosin Y staining and scoring was performed as previously documented (17).

Immunohistochemistry

Murine and human colon sections were fixed in cold acetone ($-20°C$) for 10 min and air-dried for 5 min. Blocked sections were incubated at 4°C overnight in goat anti-MRP2 polyclonal antibody (Santa Cruz Biotechnology, Santa Cruz, CA) diluted 1:750 or 1:250 in Tris-buffered saline (TBS) for mouse and human tissue, respectively. Sections were washed in TBS, followed by a 1 h incubation with fluorescein isothiocyanate (FITC)-conjugated donkey anti-goat antibody (Santa Cruz Biotechnology, Santa Cruz, CA) diluted 1:1000 and 1:250 in TBS for mouse and human sections, respectively. Sections were mounted with 1:1 1M Tris-HCl (pH 8.0)/Vectashield (Vector Laboratories, Burlingame, CA) mixture and analyzed by immunofluorescent microscopy at 20 x oil magnification (Nikon Eclipse TE-2000S).

Determination of MRP2 activity in Sf9 cells

This assay was performed according to manufacturer's instructions using membrane product SB-MRP2-SF9-ATPase (Solvo Biotechnology, Hungary). ATPase activity of the substrates probenecid (1 mM, Biomol, Plymouth Meeting, PA) and hepoxilin A_3(1, 10, 100 μM, Biomol, Plymouth Meeting, PA) was measured with respect to baseline activity.

MRP2 functional studies

Cells were treated with 10 μM CMFDA (5-chloromethylfluorescein diacetate; Molecular Probes, Carlsbad, CA) for 1 h to allow uptake and intracellular conversion to the fluorescent MRP substrate 5-chloromethylfluorescein (CMF) (18). CMF, actively transported by MRPs as the glutathione conjugate glutathione-methilfluorescein (GS-MF), was detected by measuring the appearance of fluorescence in the bathing solutions (ex 495 nm and em 535 nm; LS-5 spectrofluorimeter; PerkinElmer Life and Analytical Sciences, Boston, MA).

Permeability studies were conducted with T84 monolayers incubated in HBSS and used ^{3}H-mannitol (0.088 μM, 0.147 MBq) as a control probe for low permeability paracellular transport. Radioactivity was determined by liquid scintillation counting, and coefficients of permeability for probe molecules were similar to those found in the literature for viable monolayers (19). Transport experiments in the apical to basal (A→B) direction were initiated by adding 200 μl of the drug solution (CMFDA) to the donor chamber. Transport experiments in the basal to apical (B→A) direction were initiated by adding 1 ml of CMFDA to the basal chamber. At pre-determined times over the course of the experiment 100 μl samples were taken from the respective chamber and replaced with fresh HBSS. Transport studies conducted in the presence of the MRP inhibitor MK571 (100 μM with 0.2% DMSO) were carried out as above. The cumulative mass (M) of the drug transported from donor to receiver chambers was assessed over the time course of the experiment (dM/dt) using linear regression analysis. Equation 1 was used to fit the data;

$$dM/dt = p \cdot A \cdot C_0 \tag{1}$$

where p is the permeability coefficient (cm/s), A is the surface area of the Transwell membrane (0.333 cm^2), and C_0 the initial drug concentration in the donor chamber (nmol/cm^3). In all experiments the amount of drug transported from donor to receiver was ≤ 5% of the donor drug mass ensuring the validity of C_0 as a constant in equation 1.

Generation of small interfering RNA (siRNA) for suppression of MRP2 and P-gp expression

Plasmids used to generate siRNAs were constructed using the pSUPER vector (Oligoengine, Seattle, WA) using the method described by Brummelkamp *et al*. (20). Briefly, two oligonucleotides were designed incorporating a 19-nt sequence from each target transcript (shown in italics) or its reverse compliment separated by a short spacer region and a portion of the *Bgl*II or *Hin*dIII restriction sites. Oligonucleotides specific for the human gene *MDR1* encoding P-gp and a random control sequence were described previously (21). Oligonucleotides for the human gene encoding MRP2 (Genbank Accession # NM_000392) were: 5′ GATCCCC*GTATCAGGTTTGCCAGTTA*TTCAAGAGA*TAACTGGCAAACCTGATACT*TT TTGGAAA-3′ and 5′-AGCTTTTCCAAAAA*GTATCAGGTTTGCCAGTTA*TCTCTTGAAT*AACTGGCAAACCTG ATAC*GGG-3′. After annealing, double-stranded DNAs had overhanging restriction sites and were ligated into digested pSUPER and transformed into competent *E. coli* DH5a by standard methods, and plated on LB with ampicillin (50 μg/ml). Plasmids were extracted, purified (QIAprep Spin Mini-prep Kit, Qiagen, Valencia, CA) and sequenced for confirmation. Once confirmed, bulk plasmid was prepared for transfection using Qiagen Plasmid Midi Kit (Qiagen, Valencia, CA). Plasmids were transfected into HCT-8 intestinal epithelial cells using Lipofectamine 2000 (Invitogen, Carlsbad, CA) as described previously (21).

Cd45 Rb-hi IBD model

BALB/c mice and C.B-17scid/scid (SCID) mice (6-8 weeks old) were purchased from the Jackson Laboratories (Bar Harbor, ME) (BALB/c) and Massachusetts General Hospital (SCID). Colitis was induced in SCID mice by adoptive transfer of CD4$^+$CD45RB^{hi} T cells

isolated from splenic cells of BALB/c mice as described previously (22-24). Briefly, CD4+ T cells were enriched from the spleens of BALB/c mice using anti-CD4 (L3T4) MACS magnetic separation system (Miltenyi Biotec, Auburn, CA) according to the manufacturer's instruction. Enriched CD4+ T cells were then labeled with Cy-chrome conjugated anti-mouse CD4 MAb (PharMingen, San Diego, CA) and PE-conjugated anti-CD45RB MAb (PharMingen) and then sorted into a CD45RB^{hi} (highest staining 30%) fraction; sorting was performed with Mo-Flo (Cytomation). Each SCID mouse was injected intravenously with 200 µl of PBS containing 5 × 10^5 CD4$^+$CD45RB^{hi} T cells. Mice were weighed and monitored for appearance and signs of soft stool and diarrhea daily during the experimental period.

Lipoxygenase inhibitors

For 12/15-LOX inhibition, T84 cell monolayers were incubated in the presence baicalein [stock concentration at 1 mM in DMSO] in media for 48 hours at 37°C. Subsequently, *S. typhimurium* SL1344 was added to the apical surface of the T84 monolayers for 1 hour at 37° C and the cells were then washed free of non-adherent bacteria and processed for the PMN transmigration assay. For 5-LOX inhibition, the T84 cells were incubated for 24 hours in the presence of caffeic acid (stock concentration at 22 mM in DMSO). Both inhibitors were purchased form Biomol, Plymouth Meeting, PA.

Statistical analysis

PMN isolation was limited to repetitive donations by 10 different donors over the course of these experiments. Due to variation in both PMNs and transepithelial resistance between monolayers (baseline resistance of approximately 1,500 ohm cm^2), data were analyzed within an individual experiment and not between experiments. All results are expressed as the mean ± standard deviation of an individual experiment performed in triplicate. *P* values were calculated according to Student's *t* test, and values <0.05 were considered statistically significant.

Results

Blockade of MRP2 Function Inhibits PMN Transepithelial Migration

Elucidation of mechanisms governing HXA$_3$ synthesis and apical secretion could provide novel therapeutic strategies to impede and/or limit neutrophil involvement in deleterious events at epithelia associated with a number of chronic inflammatory conditions. HXA$_3$ must be secreted from the apical surface of epithelial cells to establish a chemotactic gradient across tight junction complexes in order to incite the paracellular movement of PMNs (2). Given the structural characteristics of HXA$_3$ and its strict apical secretion requirement, we considered the involvement of ABC transporters as potential substrates HXA$_3$. P-glycoprotein (P-gp) and MRP2 were promising candidates due to their localization on apical membranes of enterocytes (25-27). *In vitro* treatment of polarized human intestinal epithelial cell monolayers (T84) with inhibitors of either P-gp (cyclosporine A and verapamil) or MRP2 (probenecid and MK571) demonstrated a progressive, dose-dependent decrease in the ability of pathogenic *Salmonella enterica* Typhimurium (*S. typhimurium*) to induce HXA$_3$-mediated PMN transepithelial migration (Fig. 1). Moreover, at the maximal doses tested none of these drugs had an effect on PMN migration induced by imposed gradients of *N*-formyl-methionylleucylphenylalanine (fMLP) nor did they affect *S. typhimurium* internalization by T84 cell monolayers (data not shown). These results suggest that inhibitors of ABC transporters known to localize to the apical surface of intestinal epithelial cells block the recruitment of PMNs across epithelial cell monolayers induced by an inflammatory stimulus driven by HXA$_3$, in this case, apical infection with the enteric pathogenic *S. typhimurium*.

ABC transporter inhibitors are known to be poorly selective (28). To better define the relative roles played by P-gp and MRP2 in PMN transmigration, polarized epithelial cell monolayers were transfected with plasmids generating small interfering RNA (siRNA) for one of each of these two transporters. Decreased expression of MRP2 significantly attenuated (>80% inhibition) *S. typhimurium*-induced transepithelial PMN migration while monolayers generating siRNA specific for *MDR1* (encoding P-gp) showed PMN transmigration in response to *S. typhimurium* infection equivalent to control monolayers (Fig. 2a). Importantly, neither siRNA indirectly affected the ability of PMN to transmigrate as PMN migration in response to an imposed fMLP gradient was similar under all conditions (Fig. 2a). Modulation of MRP2 and P-gp expression by siRNA was verified by immunoblot analysis (Fig. 2b). Densitometric analysis showed a 75% decrease in MRP2 with siRNA in *S. typhimurium* infected cells and a complete loss for P-gp (data not shown). Inhibition of transepithelial PMN migration induced by *S. typhimurium* was consistent with the extent of protein reduction for MRP2 but not for P-gp (Fig. 2a and 2b), suggesting that MRP2, and not P-gp, is involved in PMN transepithelial migration.

During Inflammatory Events MRP2 is Functionally Active and is a Substrate for HXA$_3$

In polarized epithelial cells the majority of MRP transporters localize to the basolateral membrane (18,27). To examine functional MRP2 transporter expression related to inflammatory events, directional efflux of the MRP substrate 5-chloromethylfluorescein diacetate (CMFDA) from polarized epithelial cell monolayers was studied (Fig. 2c). CMFDA passively diffuses into cells where upon hydrolysis of the acetate moieties by cytosolic esterases it becomes the fluorescent MRP substrate 5-chloromethylfluorescein (CMF); CMF is actively transported by MRPs as the glutathione conjugate glutathione-methilfluorescein (GS-MF). In the baseline state, T84 cell monolayers have ~25-fold higher permeability coefficient in the apical to basolateral (A→B) direction relative to the B→A direction (20.3 ±1.04, and $0.8 \pm 0.03 \times 10^{-6}$ cm/sec, respectively). This relationship favors an overall basolateral secretion, or A→B transport, of GS-MF. Interestingly, T84 monolayers infected at their apical surface with wild-type *S. typhimurium* decreased the A→B/B→A permeability coefficient ratio to 1.8, with an 89% reduction of probe movement in the A→B direction, suggesting activation of an apical efflux pathway. Addition of the MRP2 inhibitor MK571 to T84 monolayers infected with wild-type *S. typhimurium* restored the A→B transport of GS-MF to 43% compared to controls with no effect on transport in the opposite direction. As a negative control, non-pathogenic *S. typhimurium* (VV341) only modestly reduced GS-MF transport (15%; p < 0.05). In contrast, P-gp functional activity was not increased during *S. typhimurium* infection (21).

The above results indicate that inflammatory events can enhance apical MRP2-specific efflux activity. We next sought to determine whether HXA$_3$ serves as a substrate for MRP2. Interestingly, MRP2 exhibits preference for negatively charged, hydrophobic molecules such as the eicosanoid cysteinyl leukotriene (29-32). HXA$_3$ shares these characteristics at neutral pH suggesting it fits the profile of an MRP2 substrate. Since ABC transporters hydrolyze ATP during active substrate transport, the ATPase activity of purified inside-out membrane vesicles isolated from *Spodoptera frugiperda* (Sf9) cells expressing the MRP2 transporter were examined following HXA$_3$ addition. MRP2-containing membrane vesicles exhibited a dose-dependent increase in ATPase activity in the presence of HXA$_3$ (Fig. 2d). Addition of the MRP2 substrate inhibitor, probenecid, was used as a positive control to depict maximal ATPase activity. Such data provide direct evidence that HXA$_3$ can be a substrate for MRP2.

Expression of MRP2 is Up-regulated in Acute and Chronic Models of Intestinal Inflammation

Previous studies have shown that the *S. typhimurium* effector protein SipA is required for the ability of *S. typhimurium* to induce PMN transepithelial migration (13,16,33). We examined

the role of virulence factors, such as SipA, to incite functional expression of MRP2 by comparing MRP2 expression levels following infection with either wild-type *S. typhimurium* (SL1344) or the isogenic SipA- mutant strain (EE633). Our results show that *S. typhimurium* stimulated MRP2 expression in a SipA-dependent manner (Fig. 3a and b); P-gp levels were not affected by *S. typhimurium* infection during a one hour infection (Fig. 3a). To control for specificity of SipA, we performed this assay using a commensal *E. coli* strain lacking SipA (F-18), as well as an isogenic strain of *S. typhimurium* mutated for an alternative effector protein, AvrA, that retains SipA expression. As anticipated, the AvrA mutant induces MRP2 expression (Fig. 3b), whereas *E. coli* F-18 fails to do so. Moreover, complementing with a *sipA* expressing plasmid (AJK63) restores the ability of the SipA mutant (EE633) to induce MRP2 protein expression (Fig. 3b). Thus, under these conditions *S. typhimurium* infection of T84 cell monolayers modulates MRP2 expression with no effect on P-gp expression.

Using SipA as a prototypical virulence element, we could also show its involvement in the release of HXA_3 since wild-type *S. typhimurium* elicited significantly more HXA_3 release from T84 cell monolayers compared to the SipA mutant (EE633), and this was correlated, respectively, with the ability to facilitate PMN migration (Method 1; Materials and Methods) (Fig. 3c). These results suggest that induction of intestinal inflammatory events, in this case SipA-mediated induction of HXA_3 release, stimulates MRP2 expression to provide a potential apical secretion mechanism for HXA_3. Furthermore, since 12-HETE is a biomarker for the HXA_3 biosynthetic pathway and is easily detected by LC/MS/MS, we next measured the amount of 12-HETE released from intestinal epithelial cells displaying reduced levels of MRP2 (via siRNA) during an infection with *S. typhimurium*. We found that the inhibition of 12-HETE from infected epithelial cells with reduced levels of MRP2 was at least 20% (n=2) compared to infected siRNA vector control monolayers. Similarly, 12-HETE release by *S. typhimurium*-infected was also profoundly inhibited by pharmacologic treatment with an MRP2 inhibitor (MK571 100 μM; data not shown). To further substantiate a link between MRP2 and the hepoxilin biosynthetic pathway we found that HXA_3 release (measured by Method 2; *Methods and Materials*) by infected T84 cells or HCT-8 cells was inhibited 55-90% (n=2) by the MRP2 inhibitor probenecid (100 μM).

We next determined whether MRP2 expression is modulated during an infection with *S. typhimurium in vivo* (16). Mice infected with wild-type *S. typhimurium* exhibited severe intestinal pathology characterized by a predominant PMN cellular infiltrate and extensive tissue damage, whereas mice infected with the SipA mutant demonstrated only a slight level of intestinal inflammation (Fig. 4a-c). Apical localization of the ABC transporter MRP2 was uniformly increased at the villus tips during the acute phase of intestinal inflammation (Fig. 4d-f), confirming MRP2 up-regulation by pathogenic *S. typhimurium*. In contrast, P-gp was not upregulated (data not shown and (21)). Collectively, this data is consistent with our *in vitro* findings suggesting MRP2 may play a role in acute salmonellosis.

Although chronic inflammatory diseases have been correlated with excessive PMN recruitment and destruction of protective epithelial barriers, many aspects of events that initiate and perpetuate PMN transmigration are poorly understood. However, using a mouse leukocyte-type 12/15- LOX antibody, an earlier study by Shannon *et al*. recognized a fundamental change in the pattern of 12/15-LOX expression in colonic tissue during onset of inflammatory bowel disease (IBD); inflamed colonic tissue expressed increased levels of 12-LOX with a corresponding increase in 12-LOX activity relative to healthy colonic tissue (34). However, there are four enzymes known to possess significant 12-LOX activity in humans: platelet-type 12-LOX (ALOX12), 12(R)-LOX (ALOX12B), epidermis-type-LOX (ALOXE3), and 15-lipoxygenase type 1 (ALOX15) (35-37) (38). 15-LOX type 1 is the human homologue of murine leukocyte type 12/15-LOX (39), and we have previously shown that PMN transepithelial migration in response to infection with *S. typhimurium* is dependent on 12/15-

LOX activity (2,9). Formation of 12-H(p)ETE by these lipoxygenases is the first step for the formation of HXA_3 (40).

To delineate the *in vivo* relevance of the above findings during chronic states of inflammation, we sought to determine whether 12-LOX inhibition blocks inflammatory outcomes associated with an IBD model induced by transfer of CD4+ CD45RB[HI] T cells (41,42). The CD4+ CD45RB[HI] T cell transfer model of IBD is well characterized, has a requirement for intestinal microorganisms, and involves the full spectrum of the immuno-inflammatory cascade, including the infiltration of PMN to the intestinal mucosa. Following disease induction, inhibition of the 12/15-LOX activity (baicalein administration by intraperitoneal injection every other day for 17 days) resulted in complete resolution of gross morphological changes, including rectal prolapse (Fig. 4g-i). This improvement was consistent with histopathology results (Fig. 4j-l). As shown in Table 1, quantification of these findings revealed that colons from PBS-treated (control) mice exhibited mucosal erosion, mucosal wall thickening and moderate crypt abcessation with an accompanying inflammatory infiltrate. In contrast, the degree of colonic inflammation in the baicalein-treated cohort was significantly decreased and the neutrophilic infiltrate returned to control levels following baicalein treatment (Fig. 4m). These results demonstrate that the severity of mucosal inflammation induced in the CD4+ CD45RB[HI] T cell transfer model of IBD was significantly attenuated by the 12/15-LOX inhibitor baicalein, which acts to prevent the synthesis of HXA_3. We were not able to perform similar experiments using either one of the MRP2-selective inhibitors since injection or oral delivery did not result in topical delivery to the colon, the required site of action.

We next posed the question of whether the 12/15-LOX activity and MRP2 expression might be coordinated as a regulated element of response to an inflammatory signal. In the presence of the 12/15-LOX inhibitor baicalein, *S. typhimurium*-infected monolayers *in vitro* showed significantly lower levels of MRP2 than those induced by this pathogen in the absence of the inhibitor (Fig. 5a). Similar treatment with caffeic acid, a 5-LOX inhibitor, failed to affect enhanced MRP2 expression induced by *S. typhimurium* infection (data not shown). Examination of intestinal tissues from CD45RB[HI] T cell transfer mice revealed that therapeutic intervention with baicalein reduced apical membrane MRP2 expression (Fig. 5b), suggesting a link between the regulation of 12/15-LOX activity and MRP2 expression during both acute and chronic inflammatory events. Taken together, these results imply that the 12/15-LOX pathway is required for maximal induction of MRP2 expression associated with epithelial inflammation.

To determine the *in vivo* relevancy of the above findings with respect to non-pathogen induced human disease we assessed whether MRP2 is up-regulated in patients with IBD. Indeed, as shown in Figure 5c, we provide direct evidence demonstrating that intestinal biopsy specimens obtained from IBD patients with either active Crohn's disease or ulcerative colitis exhibit marked MRP2 up-regulation at the intestinal epithelial apical surface compared to healthy intestinal segments. One hundred percent of the ulcerative colitis patients (4/4) and 50 percent of the Crohn's disease patients (2/4) examined in this study demonstrated an up-regulation of MRP2. None of the age and sex matched control biopsies showed any increase above baseline levels (Figure 5c).

Discussion

Given that migration of PMNs across mucosal surfaces contributes to epithelial cell dysfunction in a host of mucosal diseases (2,7,8,12), the data provided here not only identify a new mechanism underlying the vectored release of HXA_3 but also reveal interference with HXA_3 synthesis or apical secretion from epithelial cells as novel therapeutic strategies for the treatment of mucosal inflammatory disorders such as IBD. We used *S. typhimurium* as a tool

to induce an acute intestinal inflammatory response and found that during active states of intestinal inflammation apical expression of the efflux transporter MRP2 is profoundly up-regulated, functionally active, and capable of using HXA_3 as a substrate. The molecular basis of this observation is consistent with the role of the *S. typhimurium* type III secreted product SipA, as this effector protein has been found to be both necessary and sufficient for induction of PMN transepithelial migration across model intestinal epithelia (13). In keeping with its role as a virulence factor, our data now reveal that SipA mediates PMN transepithelial migration by directly affecting the release of HXA_3 via modulation of MRP2 expression. Thus, identification of the molecular mechanism by which SipA activates PMN transepithelial migration through MRP2 defines a novel pro-inflammatory signaling cascade essential for the pathogenesis of *S. typhimurium* that likely represents a paradigm of mucosal pathogen-elicited events.

Insights into pathogen-elicited active inflammation of the intestine may provide important information relating to mechanisms of disorders underlying IBD, which appear to be unrelated to pathogen colonization (43). Therefore, we hypothesize that while evolution of such responses most likely targeted pathogens such as *S. typhimurium*, aberrant activation of such pathways may lead to induction of mucosal inflammation associated with some chronic diseases of the intestine and airway. Consistent with this notion, we found a profound up-regulation of MRP2 at the apical surface of the colonic epithelium in murine models of chronic intestinal inflammation as well as in intestinal biopsies from patients presenting with active Crohn's disease and ulcerative colitis. Under normal healthy conditions, the most abundant constitutive expression of human and rat MRP2/*MRP2* mRNA is found in the renal proximal tubule brush-border membrane and the hepatocyte canalicular membrane (44). Significantly lower levels of MRP2 have been found in the small intestine with exclusive localization at the apical brush border membrane of villi (44). Further, MRP2 expression decreases in intensity from the villus tip to the crypts, where no expression has been observed (44). At this location, MRP2 is thought to play an important role in drug disposition. We now describe an unanticipated function of MRP2 as it is uniformly up-regulated at the villus tips of the apical surface of epithelial cells during active states of inflammation and plays a pivotal role in the inflammatory response.

Secreted HXA_3 then establishes a gradient through the tight junction complex to provide a chemotactic gradient used by PMNs to target the lumen of mucosal tissues at sites of inflammation (2). The observation that HXA_3 can serve as a substrate for the apical efflux transporter MRP2 fits well with the appreciation that other eicosanoids such as the cysteinyl leukotriene, LTC_4, a metabolite of the 5-LOX pathway, is one of the highest affinity MRP2 substrates characterized to date (29-32). Detailed studies, however, are required to fully characterize and provide direct evidence for MRP2 transport of hepoxilin.

There are four enzymes that possess 12-LOX activity in humans and the most abundant LOX expressed in epithelial cells is 12/15-LOX. In humans, unlike mice, 12HpETE is not the major product of 12/15-LOX (ALOX15, 4:1 ratio of 15-H(p)ETE:12-H(p)ETE) (45,46). However, 12/15-LOX is highly expressed in epithelial cells, including intestinal epithelial cells (45,46), and the synthesis of 12-HpETE through this pathway is likely significant. At present it is unclear which 12-LOX enzymes specifically contribute to HXA_3 production in the human mucosa, and thus the potential contribution of ALOX12, ALOX12B or ALOXE3 cannot be excluded. Our studies, however, determined that pharmacological inhibition of 12/15-LOX activity (both *in vitro* and *in vivo*) was found to not only block HXA_3 synthesis but also the enhanced apical expression of MRP2 typically observed as part of the inflammatory process.

Our observation that 12/15-LOX activity is coupled to MRP2 up-regulation and apical localization implies that either a metabolite of the 12/15-LOX pathway or an active form of

the enzyme itself participates in MRP2-related cellular changes associated with inflammation. However, it is unclear at this point in our investigation at what level or through what mechanism this association is achieved. Nevertheless, prior studies have demonstrated cyclooxygenase-2 expression enhances the functional activity of P-gp, providing a precedent of a causal link between arachidonic acid metabolism and expression of an ABC transporter (47). Furthermore, given that epithelial cells appear to regulate 12/15-LOX and MRP2 expression in a coupled fashion, several novel therapeutic strategies are potentially available to treat inflammatory conditions, such as IBD, based upon regulation of 12/15-LOX and MRP2. Underscoring such important clinical implications, we show that treatment with baicalein, a 12-LOX inhibitor, which inhibits HXA_3 synthesis as well as the enhanced apical expression of MRP2, resolved PMN transmigration/intestinal inflammation in a murine model of IBD.

Although our studies provide the first description that MRP2 is involved in the mechanisms that promote active states of intestinal inflammation (i.e. PMN recruitment), other ABC transporters, namely P-gp (MDR1), have been found to play a role in the development of colitis (48), albeit by a completely different mechanism than MRP2. Consistent with this observation, we have recently determined that prolonged apical colonization of intestinal epithelial cells by wild-type *S. typhimurium* (~4 h) leads not only to a profound functional decrease in P-gp but that the presence of P-gp adversely influences the ability of *S. typhimurium* to invade host cells (21). These results demonstrate that MRP2 and P-gp can be differentially regulated within the same tissue during a disease process. This observation supports the finding that during the progression of chronic renal failure MRP2 is up-regulated in both the kidney and liver, whereas P-gp remains unaffected (49).

In summary, we are beginning to understand how the PMN chemoattractant HXA_3 is secreted in a vectoral fashion through a unique efflux transport system located at the apical surface of the intestinal epithelium that involves the ABC transporter MRP2. This study demonstrates a critical link between apically-expressed MRP2 and the HXA_3 biosynthetic pathway. Surprisingly, inhibition of an enzyme critical for the synthesis of HXA_3, 12/15-LOX, was found to also suppress the apical expression of MRP2 induced by inflammatory signals. This unanticipated coupling of 12/15-LOX and MRP2 identified in an *in vitro* acute inflammatory model initiated by a pathogen was recapitulated in an *in vivo* mouse model of IBD and was consistent with observations made in biopsy samples obtained from IBD patients. Since HXA_3 has also been shown to be involved in pathogen-induced inflammation of both intestinal (2,9) and pulmonary (7) epithelial cells, it is likely that our results describe a generalized mechanism governing HXA_3 synthesis and its subsequent apical release that could provide novel therapeutic strategies to impede and/or limit PMN involvement in deleterious events associated with a number of acute and chronic inflammatory conditions.

Acknowledgements

Nonstandard abbreviations

(PMN), Neutrophil
(HXA$_3$), Hepoxilin A$_3$
(LOX), Lipoxygenase

(ABC), ATP binding cassette

(P-gp), P-glycoprotein

(*S. typhimurium*), *Salmonella enterica* serotype Typhimurium

(MRP), Multi-drug resistance associated protein

(MDR), Multi-drug resistance

(fMLP), N-formyl-methionylleucylphenylalanine

(IBD), Inflammatory bowel disease

(siRNA), Small interfering RNA

References

1. McCormick BA, Hofman PM, Kim J, Carnes DK, Miller SI, Madara JL. Surface attachment of Salmonella typhimurium to intestinal epithelia imprints the subepithelial matrix with gradients chemotactic for neutrophils. J Cell Biol 1995;131:1599–1608. [PubMed: 8522615]

2. Mrsny RJ, Gewirtz AT, Siccardi D, Savidge T, Hurley BP, Madara JL, McCormick BA. Identification of hepoxilin A3 in inflammatory events: a required role in neutrophil migration across intestinal epithelia. Proc Natl Acad Sci U S A 2004;101:7421–7426. [PubMed: 15123795]

3. Pace-Asciak CR, Reynaud D, Demin P, Nigam S. The hepoxilins. A review. Adv Exp Med Biol 1999;447:123–132. [PubMed: 10086189]

4. Nigam S, Zafiriou MP, Deva R, Ciccoli R, Roux-Van der Merwe R. Structure, biochemistry and biology of hepoxilins: an update. Febs J 2007;274:3503–3512. [PubMed: 17608719]

5. Nigam S, Patabhiraman S, Ciccoli R, Ishdorj G, Schwarz K, Petrucev B, Kuhn H, Haeggstrom JZ. The rat leukocyte-type 12-lipoxygenase exhibits an intrinsic hepoxilin A3 synthase activity. J Biol Chem 2004;279:29023–29030. [PubMed: 15123652]

6. Yu Z, Schneider C, Boeglin WE, Marnett LJ, Brash AR. The lipoxygenase gene ALOXE3 implicated in skin differentiation encodes a hydroperoxide isomerase. Proc Natl Acad Sci U S A 2003;100:9162–9167. [PubMed: 12881489]

7. Hurley BP, Siccardi D, Mrsny RJ, McCormick BA. Polymorphonuclear cell transmigration induced by Pseudomonas aeruginosa requires the eicosanoid hepoxilin A3. J Immunol 2004;173:5712–5720. [PubMed: 15494523]

8. Hurley BP, Sin A, McCormick BA. Adhesion molecules involved in hepoxilin A3-mediated neutrophil transepithelial migration. Clin Exp Immunol 2008;151:297–305. [PubMed: 18005361]

9. Mumy KL, Bien JD, Pazos MA, Gronert K, Hurley BP, McCormick BA. Distinct Isoforms of Phospholipase A2 mediate the ability of Salmonella enterica serotype Typhimurium and Shigella flexneri to induce the transepithelial migration of neutrophils. Infect Immun 2008;76:3614–3627. [PubMed: 18505810]

10. McCormick BA, Parkos CA, Colgan SP, Carnes DK, Madara JL. Apical secretion of a pathogen-elicited epithelial chemoattractant activity in response to surface colonization of intestinal epithelia by Salmonella typhimurium. J Immunol 1998;160:455–466. [PubMed: 9552004]

11. Wakabayashi K, Tamura A, Saito H, Onishi Y, Ishikawa T. Human ABC transporter ABCG2 in xenobiotic protection and redox biology. Drug Metab Rev 2006;38:371–391. [PubMed: 16877258]

12. McCormick BA, Colgan SP, Delp-Archer C, Miller SI, Madara JL. Salmonella typhimurium attachment to human intestinal epithelial monolayers: transcellular signalling to subepithelial neutrophils. J Cell Biol 1993;123:895–907. [PubMed: 8227148]

13. Lee CA, Silva M, Siber AM, Kelly AJ, Galyov E, McCormick BA. A secreted Salmonella protein induces a proinflammatory response in epithelial cells, which promotes neutrophil migration. Proc Natl Acad Sci U S A 2000;97:12283–12288. [PubMed: 11050248]

14. Gronert K, Clish CB, Romano M, Serhan CN. Transcellular regulation of eicosanoid biosynthesis. Methods Mol Biol 1999;120:119–144. [PubMed: 10343315]

15. Murphy RC, Barkley RM, Zemski Berry K, Hankin J, Harrison K, Johnson C, Krank J, McAnoy A, Uhlson C, Zarini S. Electrospray ionization and tandem mass spectrometry of eicosanoids. Anal Biochem 2005;346:1–42. [PubMed: 15961057]

16. Barthel M, Hapfelmeier S, Quintanilla-Martinez L, Kremer M, Rohde M, Hogardt M, Pfeffer K, Russmann H, Hardt WD. Pretreatment of mice with streptomycin provides a Salmonella enterica

serovar Typhimurium colitis model that allows analysis of both pathogen and host. Infect Immun 2003;71:2839–2858. [PubMed: 12704158]

17. Chen CC, Louie S, McCormick B, Walker WA, Shi HN. Concurrent infection with an intestinal helminth parasite impairs host resistance to enteric Citrobacter rodentium and enhances Citrobacter-induced colitis in mice. Infect Immun 2005;73:5468–5481. [PubMed: 16113263]

18. Lindenmaier H, Becker M, Haefeli WE, Weiss J. Interaction of progestins with the human multidrug resistance-associated protein 2 (MRP2). Drug Metab Dispos 2005;33:1576–1579. [PubMed: 16049127]

19. Siccardi D, Kandalaft LE, Gumbleton M, McGuigan C. Stereoselective and concentration-dependent polarized epithelial permeability of a series of phosphoramidate triester prodrugs of d4T: an in vitro study in Caco-2 and Madin-Darby canine kidney cell monolayers. J Pharmacol Exp Ther 2003;307:1112–1119. [PubMed: 14557377]

20. Brummelkamp TR, Bernards R, Agami R. A system for stable expression of short interfering RNAs in mammalian cells. Science 2002;296:550–553. [PubMed: 11910072]

21. Siccardi D, Mumy KL, Wall DM, Bien JD, McCormick BA. Salmonella enterica serovar Typhimurium modulates P-glycoprotein in the intestinal epithelium. Am J Physiol Gastrointest Liver Physiol 2008;294:G1392–1400. [PubMed: 18403618]

22. Powrie F, Leach MW, Mauze S, Caddle LB, Coffman RL. Phenotypically distinct subsets of CD4+ T cells induce or protect from chronic intestinal inflammation in C. B-17 scid mice. Int Immunol 1993;5:1461–1471. [PubMed: 7903159]

23. Morrissey PJ, Charrier K, Braddy S, Liggitt D, Watson JD. CD4+ T cells that express high levels of CD45RB induce wasting disease when transferred into congenic severe combined immunodeficient mice. Disease development is prevented by cotransfer of purified CD4+ T cells. J Exp Med 1993;178:237–244. [PubMed: 8100269]

24. Totsuka T, Kanai T, Uraushihara K, Iiyama R, Yamazaki M, Akiba H, Yagita H, Okumura K, Watanabe M. Therapeutic effect of anti-OX40L and anti-TNF-alpha MAbs in a murine model of chronic colitis. Am J Physiol Gastrointest Liver Physiol 2003;284:G595–603. [PubMed: 12631559]

25. Chan LM, Lowes S, Hirst BH. The ABCs of drug transport in intestine and liver: efflux proteins limiting drug absorption and bioavailability. Eur J Pharm Sci 2004;21:25–51. [PubMed: 14706810]

26. Kullak-Ublick GA, Becker MB. Regulation of drug and bile salt transporters in liver and intestine. Drug Metab Rev 2003;35:305–317. [PubMed: 14705863]

27. Prime-Chapman HM, Fearn RA, Cooper AE, Moore V, Hirst BH. Differential multidrug resistance-associated protein 1 through 6 isoform expression and function in human intestinal epithelial Caco-2 cells. J Pharmacol Exp Ther 2004;311:476–484. [PubMed: 15210835]

28. Kruijtzer CM, Beijnen JH, Schellens JH. Improvement of oral drug treatment by temporary inhibition of drug transporters and/or cytochrome P450 in the gastrointestinal tract and liver: an overview. Oncologist 2002;7:516–530. [PubMed: 12490739]

29. Shen H, Paul S, Breuninger LM, Ciaccio PJ, Laing NM, Helt M, Tew KD, Kruh GD. Cellular and in vitro transport of glutathione conjugates by MRP. Biochemistry 1996;35:5719–5725. [PubMed: 8639531]

30. Leier I, Jedlitschky G, Buchholz U, Center M, Cole SP, Deeley RG, Keppler D. ATP-dependent glutathione disulphide transport mediated by the MRP gene-encoded conjugate export pump. Biochem J 1996;314(Pt 2):433–437. [PubMed: 8670053]

31. Muller M, Meijer C, Zaman GJ, Borst P, Scheper RJ, Mulder NH, de Vries EG, Jansen PL. Overexpression of the gene encoding the multidrug resistance-associated protein results in increased ATP-dependent glutathione S-conjugate transport. Proc Natl Acad Sci U S A 1994;91:13033–13037. [PubMed: 7809167]

32. Loe DW, Almquist KC, Deeley RG, Cole SP. Multidrug resistance protein (MRP)-mediated transport of leukotriene C4 and chemotherapeutic agents in membrane vesicles. Demonstration of glutathione-dependent vincristine transport. J Biol Chem 1996;271:9675–9682. [PubMed: 8621643]

33. Zhang S, Santos RL, Tsolis RM, Stender S, Hardt WD, Baumler AJ, Adams LG. The Salmonella enterica serotype typhimurium effector proteins SipA, SopA, SopB, SopD, and SopE2 act in concert to induce diarrhea in calves. Infect Immun 2002;70:3843–3855. [PubMed: 12065528]

34. Shannon VR, Stenson WF, Holtzman MJ. Induction of epithelial arachidonate 12-lipoxygenase at active sites of inflammatory bowel disease. Am J Physiol 1993;264:G104–111. [PubMed: 7679252]

35. Yamamoto S, Kishimoto K, Arakawa T, Suzuki H, Nakamura M, Yoshimoto T, Takao T, Shimonishi Y, Tanabe T. Arachidonate 12-lipoxygenases. Catalytic properties and regulation of the enzyme gene. Adv Exp Med Biol 1997;407:191–196. [PubMed: 9321952]

36. Yoshimoto T, Yamamoto S. Arachidonate 12-lipoxygenase. J Lipid Mediat Cell Signal 1995;12:195–212. [PubMed: 8777566]

37. Yamamoto S, Suzuki H, Nakamura M, Ishimura K. Arachidonate 12-lipoxygenase isozymes. Adv Exp Med Biol 1999;447:37–44. [PubMed: 10086181]

38. Funk CD, Chen XS, Johnson EN, Zhao L. Lipoxygenase genes and their targeted disruption. Prostaglandins Other Lipid Mediat 2002;68-69:303–312. [PubMed: 12432925]

39. Collins JF, Hu Z, Ranganathan PN, Feng D, Garrick LM, Garrick MD, Browne RW. Induction of arachidonate 12-lipoxygenase (Alox15) in intestine of iron-deficient rats correlates with the production of biologically active lipid mediators. Am J Physiol Gastrointest Liver Physiol 2008;294:G948–962. [PubMed: 18258795]

40. Pace-Asciak CR, Asotra S. Biosynthesis, catabolism, and biological properties of HPETEs, hydroperoxide derivatives of arachidonic acid. Free Radic Biol Med 1989;7:409–433. [PubMed: 2514125]

41. Mackay F, Browning JL, Lawton P, Shah SA, Comiskey M, Bhan AK, Mizoguchi E, Terhorst C, Simpson SJ. Both the lymphotoxin and tumor necrosis factor pathways are involved in experimental murine models of colitis. Gastroenterology 1998;115:1464–1475. [PubMed: 9834274]

42. Philippe D, Dubuquoy L, Groux H, Brun V, Chuoi-Mariot MT, Gaveriaux-Ruff C, Colombel JF, Kieffer BL, Desreumaux P. Anti-inflammatory properties of the mu opioid receptor support its use in the treatment of colon inflammation. J Clin Invest 2003;111:1329–1338. [PubMed: 12727924]

43. McCormick BA, Miller SI, Carnes D, Madara JL. Transepithelial signaling to neutrophils by salmonellae: a novel virulence mechanism for gastroenteritis. Infect Immun 1995;63:2302–2309. [PubMed: 7768613]

44. Van Aubel RA, Hartog A, Bindels RJ, Van Os CH, Russel FG. Expression and immunolocalization of multidrug resistance protein 2 in rabbit small intestine. Eur J Pharmacol 2000;400:195–198. [PubMed: 10988333]

45. Kuhn H, Walther M, Kuban RJ. Mammalian arachidonate 15-lipoxygenases structure, function, and biological implications. Prostaglandins Other Lipid Mediat 2002;68-69:263–290. [PubMed: 12432923]

46. Kuhn H, O'Donnell VB. Inflammation and immune regulation by 12/15-lipoxygenases. Prog Lipid Res 2006;45:334–356. [PubMed: 16678271]

47. Sorokin A. Cyclooxygenase-2: potential role in regulation of drug efflux and multidrug resistance phenotype. Curr Pharm Des 2004;10:647–657. [PubMed: 14965327]

48. Panwala CM, Jones JC, Viney JL. A novel model of inflammatory bowel disease: mice deficient for the multiple drug resistance gene, mdr1a, spontaneously develop colitis. J Immunol 1998;161:5733–5744. [PubMed: 9820555]

49. Laouari D, Yang R, Veau C, Blanke I, Friedlander G. Two apical multidrug transporters, P-gp and MRP2, are differently altered in chronic renal failure. Am J Physiol Renal Physiol 2001;280:F636–645. [PubMed: 11249855]
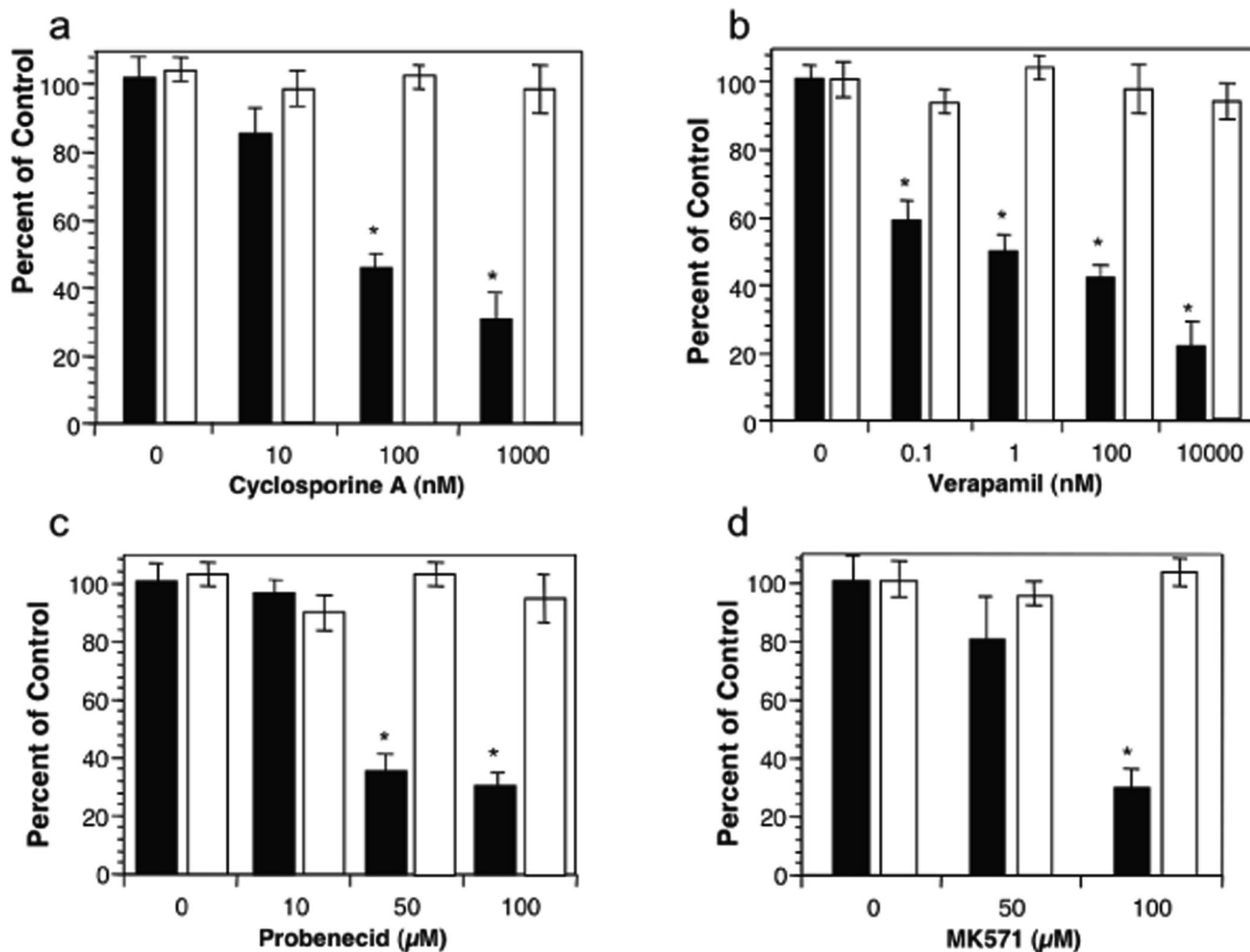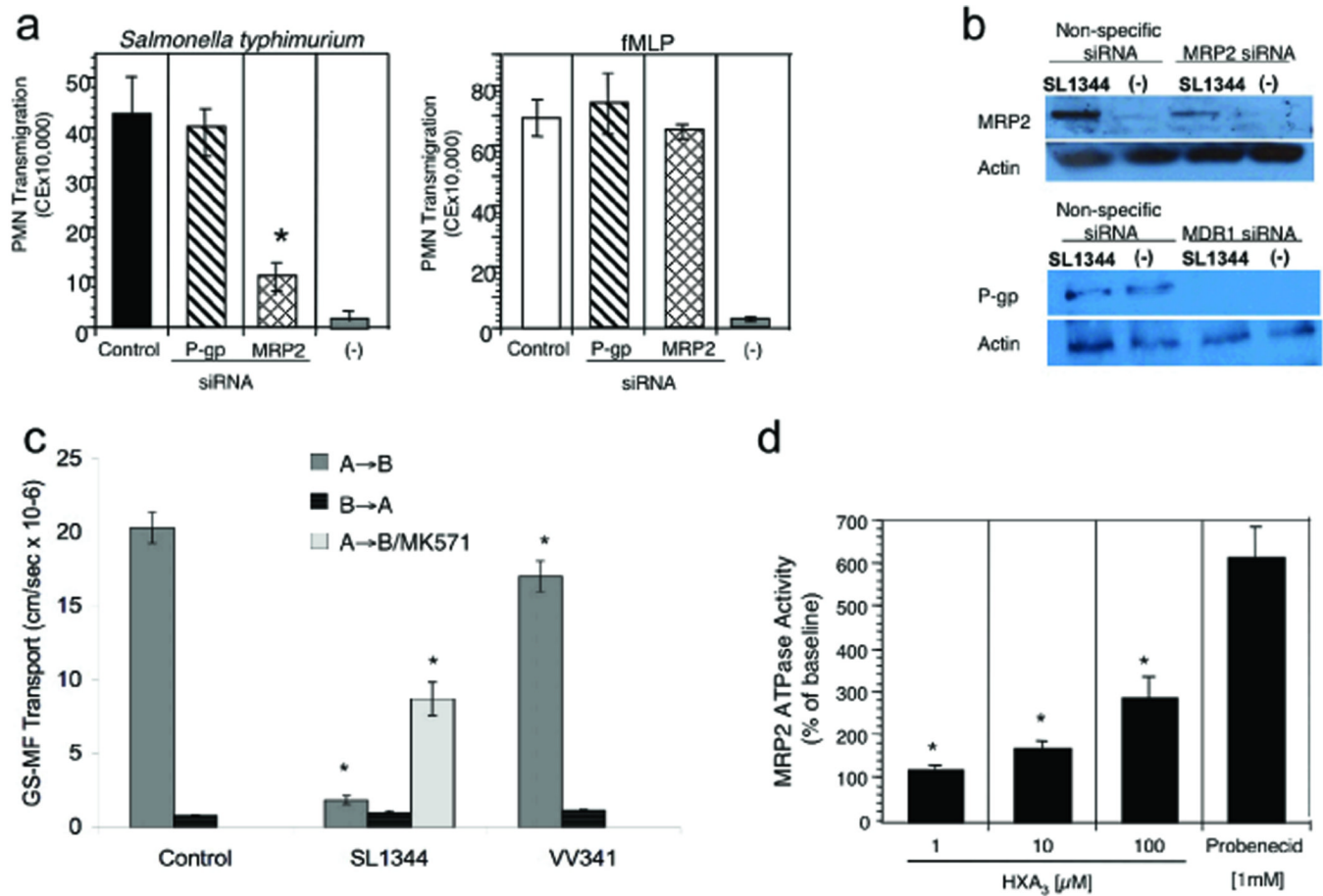
Figure 1.
The effect of P-gp (MDR1) and MRP2 inhibitors on the ability of *S. typhimurium* to induce PMN transepithelial migration. T84 cell monolayers were treated for 1 hr with the P-gp inhibitors (cyclosporine A (10-1000 nM; (a)) or verapamil (0.1-10000 nM; (b)) or the MRP2 inhibitors (probenecid (10-100 μM; (c)) or MK571 (50-100 μM; (d)). The pre-treated monolayers were then infected at the apical surface with wild-type *S. typhimurium* SL1344 and judged for their ability to induce PMN transepithelial migration (see Methods). Closed bars (black) represent *S. typhimurium* induced PMN transepithelial migration while the open bars (white) represent PMN migration to imposed gradients of fMLP. Data are expressed as the mean and SD of triplicate samples. This experiment is representative of more than three performed. * $P < 0.01$

Figure 2.
Demonstration of the functional importance of the apical ABC transporter MRP2 during PMN transepithelial migration and as a substrate for HXA$_3$. *a)* Polarized intestinal cell monolayers silenced for the expression of MRP2 or P-gp (MDR1) were assessed for the ability to promote *S. typhimurium*-induced PMN transepithelial migration. Data are represented as mean ± SD of triplicate samples and are representative of three experiments; * P < 0.01. *b)* Immunoblot analysis of the modulation in protein expression of MRP2 and P-gp (MDR1) based on siRNA, as described in the *Methods* section. Results are representative of three independent experiments. *c)* MRP2 functional activity was assessed by measuring GS-MF efflux from polarized monolayers of T84 infected in the absence and presence of *S. typhimurium.* T84 cell monolayers were infected apically for 1 h with either SL1344 (wild type *S. typhimurium*) or VV341 (an isogenic derivative of SL1344 which lacks the *hilA* gene and is invasion deficient). Control represents baseline transport in the presence of physiologic buffer (HBSS). A→B represents transport in the apical to basolateral direction; B→A represents transport in the basolateral to apical direction; MK571 is an MRP2 inhibitor (100 μM containing 2% DMSO). Data are expressed as mean ± SD of triplicate samples and are representative of at least three independent experiments; * P < 0.01. *d)* Inorganic phosphate (Pi) yielded by hydrolysis of ATP used by the substrate HXA$_3$ is represented as percent of the baseline response. Pi was measured as (nmol/mg/protein/min) and baseline values were determined to be 1.6 ± 0.15. Bars represent the mean ± SD of triplicate determinations representative of at least three independent experiments; * P < 0.05.
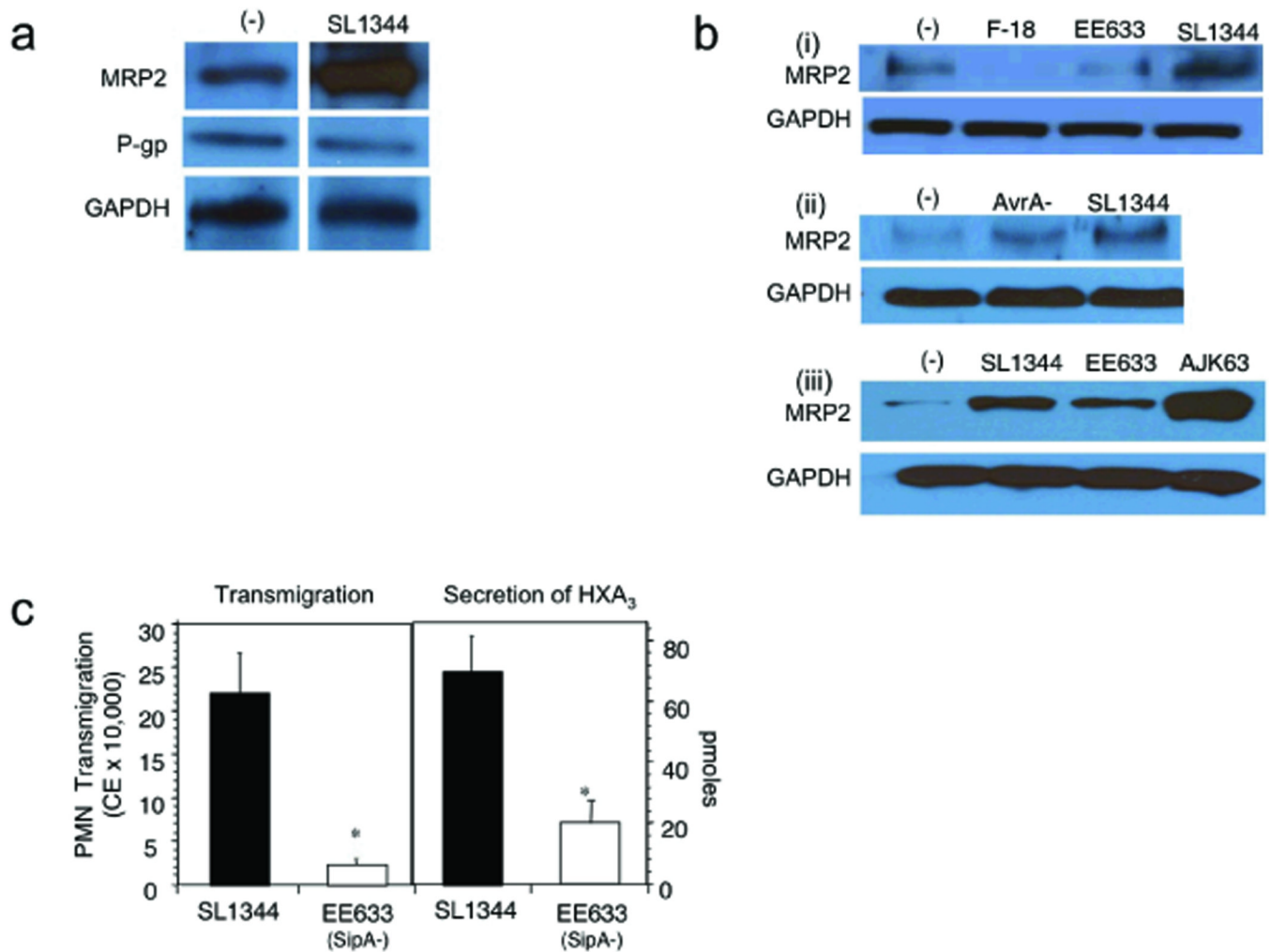
Figure 3.
MRP2 is up-regulated by an inflammatory pathway activated by *S. typhimurium* that involves a SipA dependent-mechanism. *a)* T84 cells were infected apically with SL1344 for 1 h, then lysed, and enriched for the TX-100 insoluble membrane fraction as described under *Methods*. Incubation with the physiologic buffer HBSS served as the baseline control for MRP2 expression. 25 μg of protein was separated on a 10% polyacrylamide PAGE gel and immunoblotted for MRP2. *b)* To determine specificity of the response (i) T84 cell monolayers were apically infected with SL1344, the isogenic SipA mutant strain (EE633), and a normal intestinal human flora *E. coli* isolate, *E. coli* F-18, or left uninfected in the presence of HBSS ((−) control). (ii) T84 cells were infected apically for 1 h in the presence of either SL1344 or its isogenic AvrA (*S. typhimurium* effector protein) mutant strain. (−) represents the baseline buffer control. (iii) T84 cell monolayers were apically infected for 1 h in the presence of SL1344, EE633, or the *sipA* complemented strain AJK63. This strain is derived from EE633 containing the pAK68C plasmid that encodes *sipA*. (−) represents the baseline buffer control. For each immunoblot, following bacterial infection the cells were lysed and then enriched for the TX-100 insoluble membrane fraction. 25 μg of protein was separated on 10% polyacrylamide PAGE gels and immunoblotted for MRP2. The data represent a single experiment and are repetitive of at least three experiments performed. *c)* SipA affects the release of HXA$_3$ from model intestinal epithelia. Monolayers of T84 epithelial cells were infected for 1 h with SL1344 or EE633 *S. typhimurium* strain. PMN transepithelial cell

migration (left) and HXA$_3$ secretion (right) were measured. HXA$_3$ was identified according to Method 1 as described in *Methods and Materials*. Data are presented as the mean ± SD of assays performed in triplicate and are representative of three independent experiments; *P < 0.01.
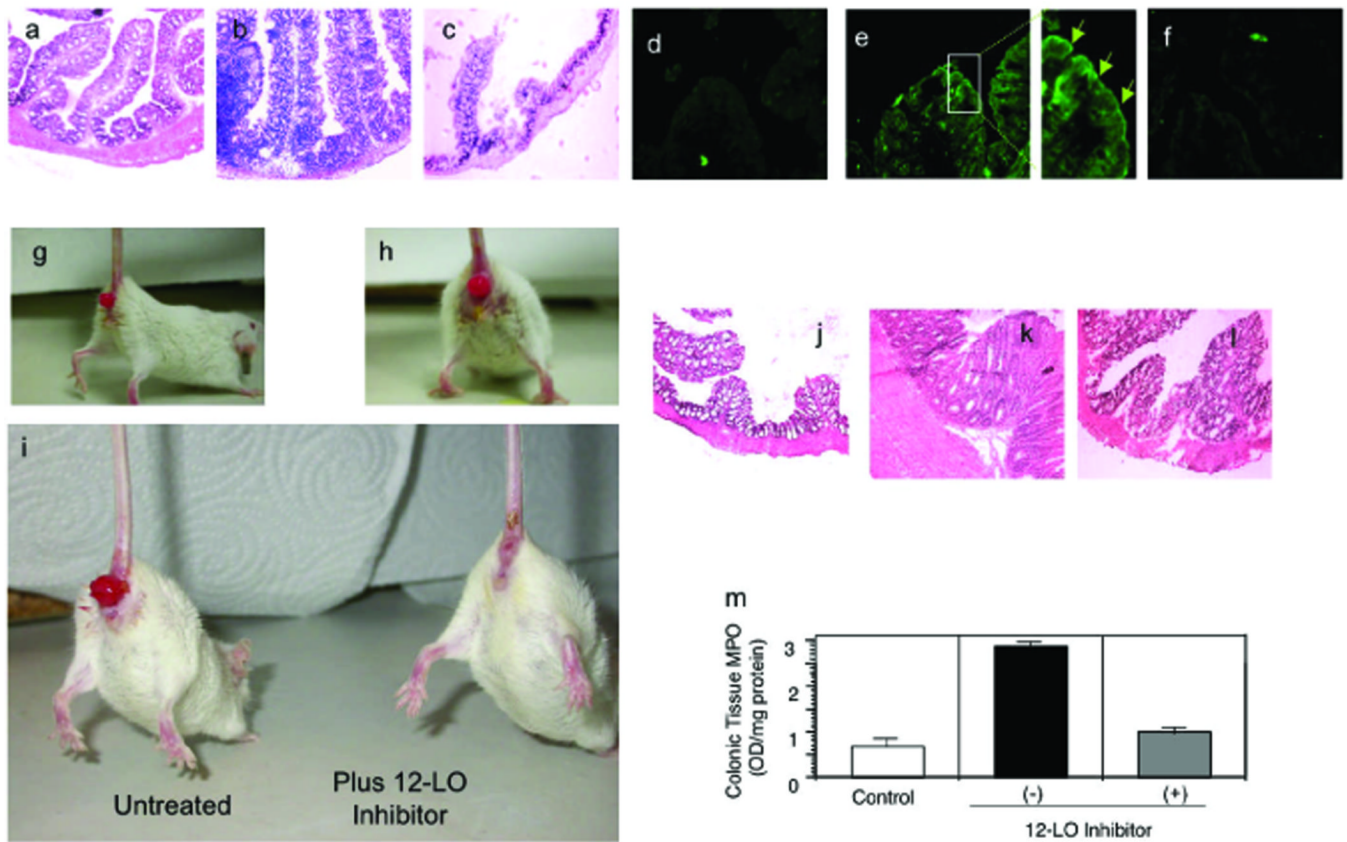
Figure 4.
MRP2 expression is modulated during active states of intestinal inflammation. *a-c)*
Histopathology of the proximal large colon of mice following a 48 h infection with physiologic
buffer (HBSS; *a*), SL1344 (*b*), and EE633 (*c*). Sections are stained with hemotoxylin and eosin
(H and E) and represent a magnification of 20X. *d-f)* Immunohistochemistry of the expression
pattern of MRP2 in the proximal large colon performed on the same set of mice described for
a-c. Panels *d, e, f* represent buffer control, SL1344, and EE633 infected mice, respectively;
10X magnification. The enhanced boxed image in panel *e* illustrates the apical expression of
MRP2 as denoted by the green arrows. *g* and *h)* Gross examination of the anal region in mice
induced to exhibit characteristics of IBD using the CD4+ CD45RB^{hi} T cell adoptive transfer
model. Following induction of disease the mice generally exhibit significant rectal prolapse.
i) Gross examination of the diseased mice (CD4+ CD45RB^{hi} T cell adoptive transfer model)
following a therapeutic intervention strategy using the 12/15-LOX inhibitor baicalein. *j-l)* H
and E stained proximal colonic sections of mice not induced for IBD (*j*), mice induced for IBD
(*k*), and mice induced for disease and then therapeutically treated with baicalein (*l*); 20X
magnification. *m)* PMN infiltration into the proximal colon quantified by tissue
myeloperoxidase (MPO). Data are expressed as the mean ± SD and represent groups of five
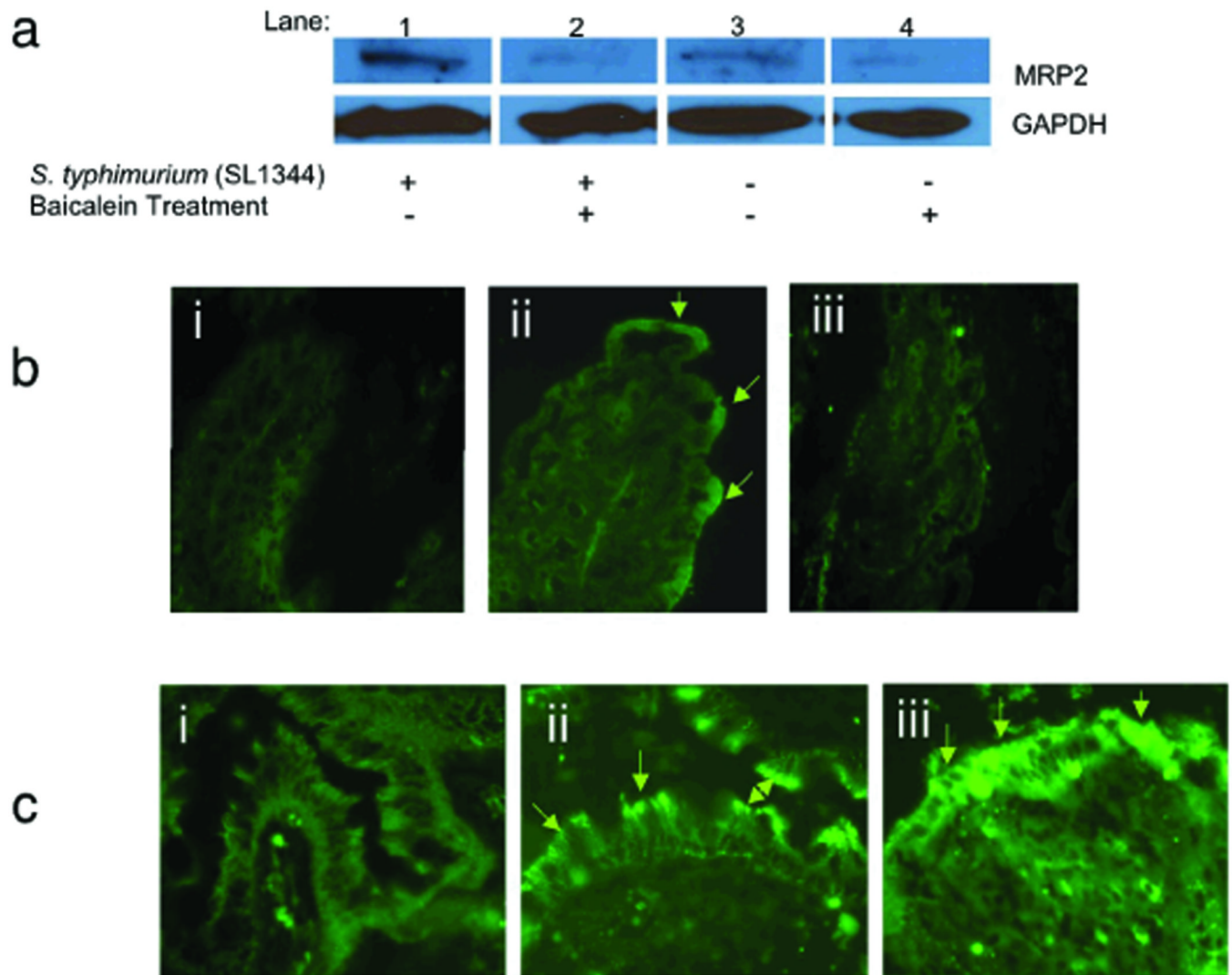mice per data set and the experiment was performed three times with similar results.

Figure 5.
12/15-LOX activity and the expression of MRP2 are linked events in response to active states of intestinal inflammation. *a)* Immunoblot analysis of MRP2 expression during apical infection of SL1344 in the absence and presence of the 12-LOX inhibitor baicalein, as described in *Methods*. For each sample 25 μg of protein was isolated from the membrane fraction and run on a 10% polyacrylamide PAGE gel and immunoblotted for MRP2. The data represent a single experiment and are repetitive of at least three experiments performed. *b)* Immunohistochemistry depicting the localization of MRP2 to the apical epithelial surface of the proximal colon in mice treated in the absence and presence of 12/15-LOX inhibition using the CD4+ CD45RB^{hi} T cell adoptive transfer model of IBD: (i) represents the healthy control which did not undergo the adoptive transfer of the CD4+ CD45RB^{hi} T cells; (ii) represents mice induced for IBD; and; (iii) represents mice induced for IBD and then therapeutically treated with baicalein. 10X magnification. c) Human intestinal biopsy specimens stained for MRP2: (i) healthy colonic section; (ii) colonic section from a patient with active Crohn's disease, (iii); colonic section from a patient with active ulcerative colitis (20X magnification). Data represent a single experiment that is representative of eight patient colonic biopsy specimens examined (four each for Crohn's and ulcerative colitis patients).

Table 1

Quantification of Intestinal Inflammation

	Cellular Infiltration[a]	Tissue Damage[a]	Total Inflammation Score[b]
Normal control	0.25 ± 0.11	0.18 ± 0.05	0.43 ± 0.17
Untreated	3 ± 0.81	2.75 ± 0.85	5.75 ± 1.50
12-LOX inhibitor	1 ± 0.10	1.5 ± 0.70	2.5 ± 0.70

Quantification of the severity of intestinal inflammation in mice treated in the absence and presence of the 12/15-LOX inhibitor baicalein. Disease scores of colonic inflammation are assessed by determination of infiltration of inflammatory cells (range 0-4)[a] together with the evaluation of colonic damage, including edema (range 0-4)[a]. The combined score represents the total inflammatory score (maximum = 8)[b]. Five animals were used per experimental treatment condition and the experiment was performed three times.